ANTERIOR VS POSTERIOR PURKINJE CELL FIRING RATE ANALYSIS: INSIGHTS FROM THE RAT CEREBELLUM

Brune Bettler
WINTER 2024

Laboratory in Neurobiology
BIOL 389

Abstract:

The cerebellum is necessary for sensorimotor coordination across all vertebrates and plays a role in various cognitive functions in humans. The degeneration of the intrinsic firing patterns of its output, in the form of Purkinje cell spiking, is the cause of numerous diseases and behavioral abnormalities. This study investigates the differences in Purkinje cell firing patterns between the anterior and posterior zones of the rat vermis in vitro. Our findings reveal that while the mean dominant firing frequencies of Purkinje cells in these zones did not significantly differ, the coefficient of variation (CV) in firing rates was significantly higher in the posterior zone. Additionally, analysis of inter-spike intervals showed distinct patterns, with posterior cells exhibiting frequency 'jumps' and a broader distribution of intervals compared to anterior cells. These results highlight the intrinsic firing differences between the anterior and posterior vermis Purkinje cells, paving the way toward a greater understanding of cerebellar function and dysfunction.

Introduction:

The cerebellum is a highly conserved structure in the vertebrate brain responsible for sensorimotor coordination (Sultan & Glickstein, 2007). It receives input from different sensory modalities and body positions and integrates these to predict and execute future movements. Due to its dense neuronal population, distinct cell types, and characteristic circuitry, the cerebellum was previously hypothesized to house a “single computation” (Diedrichsen et al., 2019). However, the emerging complex roles of the cerebellum in certain learning and cognitive functions including speech and memory, as

well as the interconnectedness of the cerebellum and the cerebral cortex in humans, suggest much more nuanced computations (Welniarz et al., 2021), (Carey, 2024).

The intrinsic structural and functional differences within the cerebellum itself may be the basis for its complex role in many behaviors and processes. Structural and functional abnormalities of the cerebellum are linked to ataxia, vision and speech dysfunction, tremors, balance issues, and autism spectrum disorders (Carey, 2024). Many diseases also show deficits of typical molecular patterning in the cerebellum (Toscano Márquez et al., 2021). Notably, the expression of the biomarker Zebrin II, which is naturally expressed in stripes across the cerebellar vermis, influences the firing properties and synaptic plasticity of Purkinje cells (Lehman et al., 2020). These cells are inhibitory neurons that constitute the sole output of the cerebellum and reflect its computations. Purkinje cells fire intrinsically at high frequencies up to 200Hz and are essential for cerebellar function. Disruptions in their activity have been linked to various cerebellar diseases and rescuing their intrinsic activity may be sufficient to restore impaired behavior (Cook et al., 2021). As such, studying and characterizing the differences in Purkinje firing patterns and spike synchronization could be fundamental to understanding more about cerebellar diseases and the functioning of the vertebrate brain as a whole.

In mammals, the vermis is located in the medial portion of the two cerebellar hemispheres. Its inputs from the cerebral cortex and the importance of its outputs for the coordination of central body and proximal limb movements, make the vermis an ideal region for studying the regional differences in output Purkinje firing patterns (Unverdi & Alsayouri, 2024), (Coffman et al., 2011). This region is anatomically divided

by the primary fissure into anterior (lobules I-V) and posterior (lobules VI-IX) zones that each differ in susceptibility to neurodegeneration and expression of various biomarkers, including Zebrin II, which are highly conserved across all vertebrates (Lehman et al., 2020). These striped “bands' ' of differential molecular and genetic expression in the vermis result in differences in Purkinje baseline firing rates and synaptic plasticity (Carey, 2024). For example, the anterior zone of the vermis is more sensitive to damage, exhibits higher rates of Purkinje cell death, and is often the first zone to degenerate in comparison with the posterior zone (Hernández-Pérez et al., 2023).

Our research continues this exploration by studying the differences between the anterior and posterior zones of the rat vermis. Rats are ideal models for the study of the cerebellum as they have larger brains than those of other commonly used rodents such as mice, and their cerebellum shares many anatomical and functional similarities with that of humans (Wright, 2015). We hypothesize that Purkinje cells in the anterior and posterior zones will exhibit different patterns of activity, with less firing variability in the anterior zone as predicted due to their higher susceptibility to degeneration.

Method details:

P18 to P25 rats were deeply anesthetized with isoflurane and decapitated, their brains were rapidly placed in ice-cold artificial cerebrospinal fluid (ACSF, in mM: 125 NaCl, 2.5 KCl, 2 CaCl2, 1 MgCL2, 1.25 NaHPO4, 26 NaHCO3, and 20 glucose, bubbled with 95% O2-5% CO2 to maintain pH at 7.3, osmolarity of 320+\- 5 mOsm). Parasagittal acute cerebellar slices (200µm) from the vermis were prepared using a Leica VT1000S vibrating blade microtome. The slices were incubated in a dark chamber

with ACSF at 37oC for 45 minutes, followed by incubation at room temperature. We performed extracellular somatic recordings from Purkinje cells in different lobules of the cerebellar vermis with a Multiclamp 700B amplifier (Molecular Devices), at 33oC. An upright microscope (Scientifica, UK) was used to visualize Purkinje cells soma. Borosilicate patch pipettes were pulled using a P-1000 puller (Sutter Instruments, USA; ~1M) and filled with ACSF. Data acquisition and analysis were performed using custom-designed Igor Pro 8.0 acquisition software (Wavemetrics, USA).

Results:

The cerebellum is a distinct portion of the brain characterized by its intricate folds. In rats, it is located behind the cerebrum and above the brainstem (figure 1A). In this study, we sampled Purkinje cells located in the rat vermis, the central region of the cerebellum that separates the two cerebellar hemispheres (Coffman et al., 2011). As seen in Figure 1B, the primary fissure anatomically divides the vermis into two different lobules: the anterior (lobules I-V) and posterior (lobules VI-IX) zones. Recordings were made as per the methods resulting in trains of action potential spikes from n=10 anterior and n=8 posterior units. These units were isolated and determined to be Purkinje neurons (as per the methods) and will be referred to as such from now on. Two characteristic spike train sample recordings can be seen in Figure 1C. The red-colored anterior zone Purkinje spikes appear regular in comparison to the blue posterior zone Purkinje spike trains. Figure 1D contains a correlogram of both anterior (red) and posterior (blue) sample units. The X-axis represents the time lag between subsequent spikes and the Y-axis indicates spike frequency. The rhythmic half-circle pattern of the

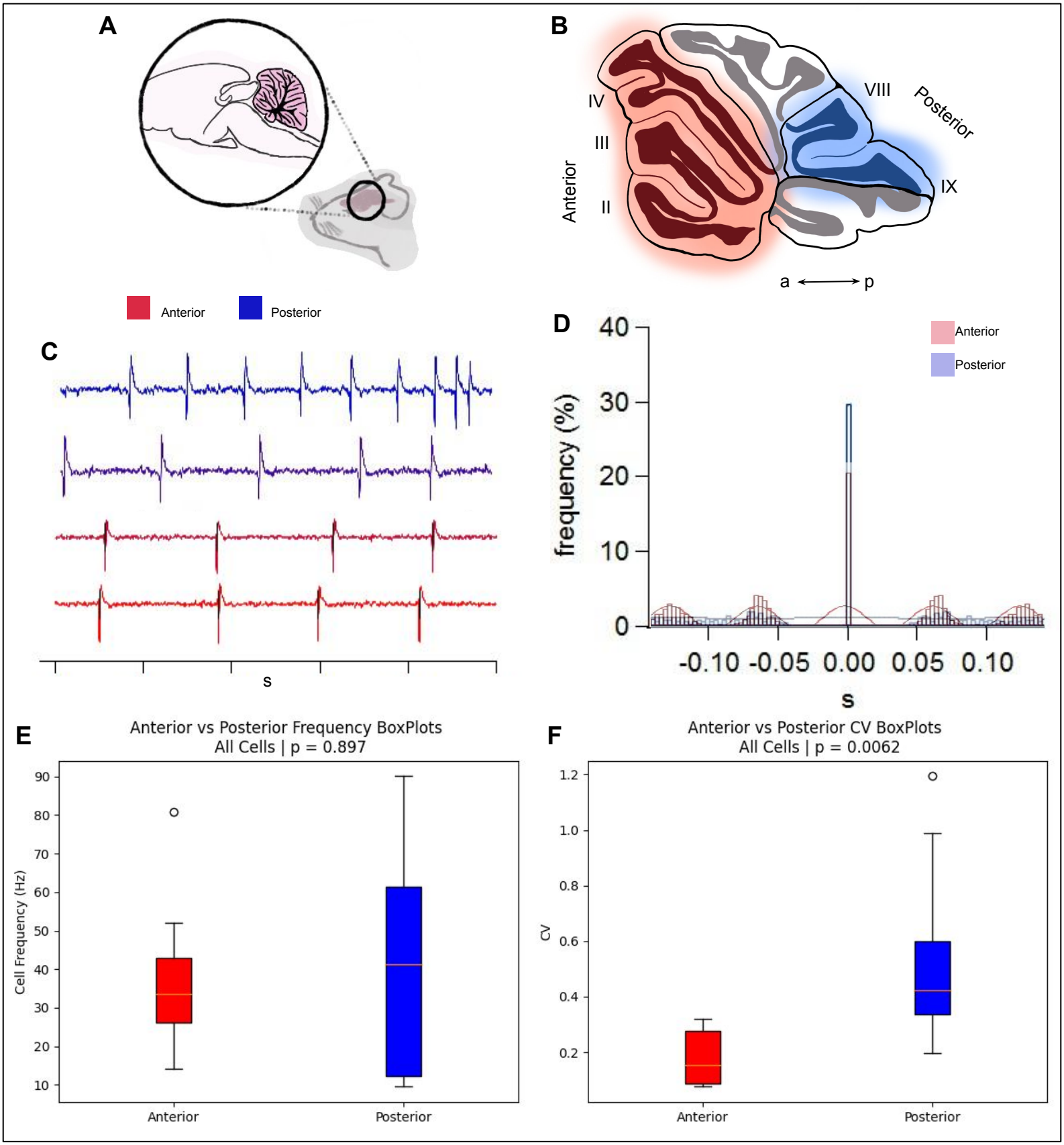

Figure 1. Overview of anterior vs posterior Purkinje cell firing patterns

(A) Diagram of a rat brain with the cerebellum highlighted in pink (modified from Biorender.com).
(B) Close-up diagram of the rat cerebellum with the lobules II, III, IV as the anterior portion of the cerebellum and lobules VIII and IX corresponding to the posterior cerebellum (modified from Hernández-Pérez et al., 2023).
(C) Example spike trains from both anterior (red) and posterior (blue) units. The time scale is in seconds.
(D) Example correlograms obtained during data recording. The colored sinusoidal colored line corresponds to the dominant frequency determined by the recording software and fit to the data.
(E) Box plots representing the dominant frequency data gathered from all n=10 anterior (red) units and n=8 posterior (blue) cells. A Mann Whitney U test was run between the data resulting in a non-significant p value of 0.897.
(F) Box plots representing the dominant CV gathered from all n=10 anterior (red) units and n=8 posterior (blue) cells. A Mann Whitney U test was run between the data resulting in a significant p value of 0.0062.

anterior unit plot (red) suggests firing synchrony and regular oscillatory firing. In contrast, the flat pattern of the posterior unit plot suggests a lack of rhythmic temporal structure.

The mean firing frequency for each neuron was determined by taking the mean of all mean frequencies recorded per spike train. The CV was calculated by dividing the standard deviation by the mean of each cell. While not always identical, this data was very similar to that of the dominant frequency and CV returned by Igor Pro 8.0 for each neuron. We chose to use our calculations rather than those of Igor Pro for consistency and for better understanding of the underlying data used. From our data, the mean dominant frequency and CV were 36.63Hz and 0.18 respectively over all recorded anterior Purkinje cells and 43.15Hz and 0.54 respectively over all recorded posterior Purkinje cells. A boxplot of mean dominant frequency values and CV for all anterior and posterior cells is shown in Figure 1E and 1F respectively. For both plots, the red plots represent anterior cell data while the blue plots represent the posterior cell data. As determined by the Mann-Whitney U test, the difference between anterior and posterior mean firing frequency was non-significant ($p = 0.897$) while the difference in CV values was significant between anterior and posterior groups ($p = 0.0062$).

To better understand underlying spike data, we then looked at the inter-spike intervals between each action potential spike for all spike trains of all recorded cells. Figures 2A (red) and 2B (blue) show the inter-spike interval values from each spike train of two example anterior and posterior neurons respectively. Each row on the plots represents one 8-second spike train. Spike trains were recorded one after the other (shown with increasingly dark color shades), though not always consecutively, and may

contain an unknown amount of seconds between them (see methods for details). From the 72 seconds of recording from anterior neuron 5, the mean frequency per spike train ranged from 13.3Hz to 16.7Hz with a CV less than or equal to 0.15 for all spike trains (figure 2A left). Anterior cell 4 had a range of 13.9Hz-52.2Hz for the mean frequencies per spike train and a CV range of 0.17-0.49 (figure 2A right). Interestingly, posterior cells sometimes exhibited “jumps” between frequencies as can be seen in Figure 2B in the first spike train of cell 8 and in Supplemental Figure 2, cell 7. While these stark jumps were not observed in any recorded anterior cells, we noticed a repetitive delay pattern in both anterior and posterior cell types in which multiple frequencies could be extracted from one spike train. This can be observed in posterior cell 2 in Figure 2B and more remarkably in anterior cell 7 in Supplemental Figure 1. All inter-spike interval plots for all anterior and posterior units not shown in Figure 2 can be found in supplementary figures 1 and 2 respectively. Posterior cell 8 had a mean frequency per spike train range of 32.8Hz-152.8Hz and a CV range of 0.26-0.64. Posterior cell 2 had a mean frequency range of 22.2Hz-53.0Hz and a CV range of 0.31-0.60. The inter-spike intervals of these two sample posterior cells can be seen in Figure 2B.

To better visualize and quantify our observations per spike train for each neuron (as opposed to “per whole-neuron” from Figure 1), we pooled together all individual spike-train inter-spike intervals. The mean frequencies and CVs for all anterior and posterior neuron spike trains were then calculated and visualized as box plots. Consistent with the whole-neuron data, anterior vs posterior per-spike train frequencies were not significantly different as per the Mann-Whitney U test (Figure 2C, $p=0.145$).

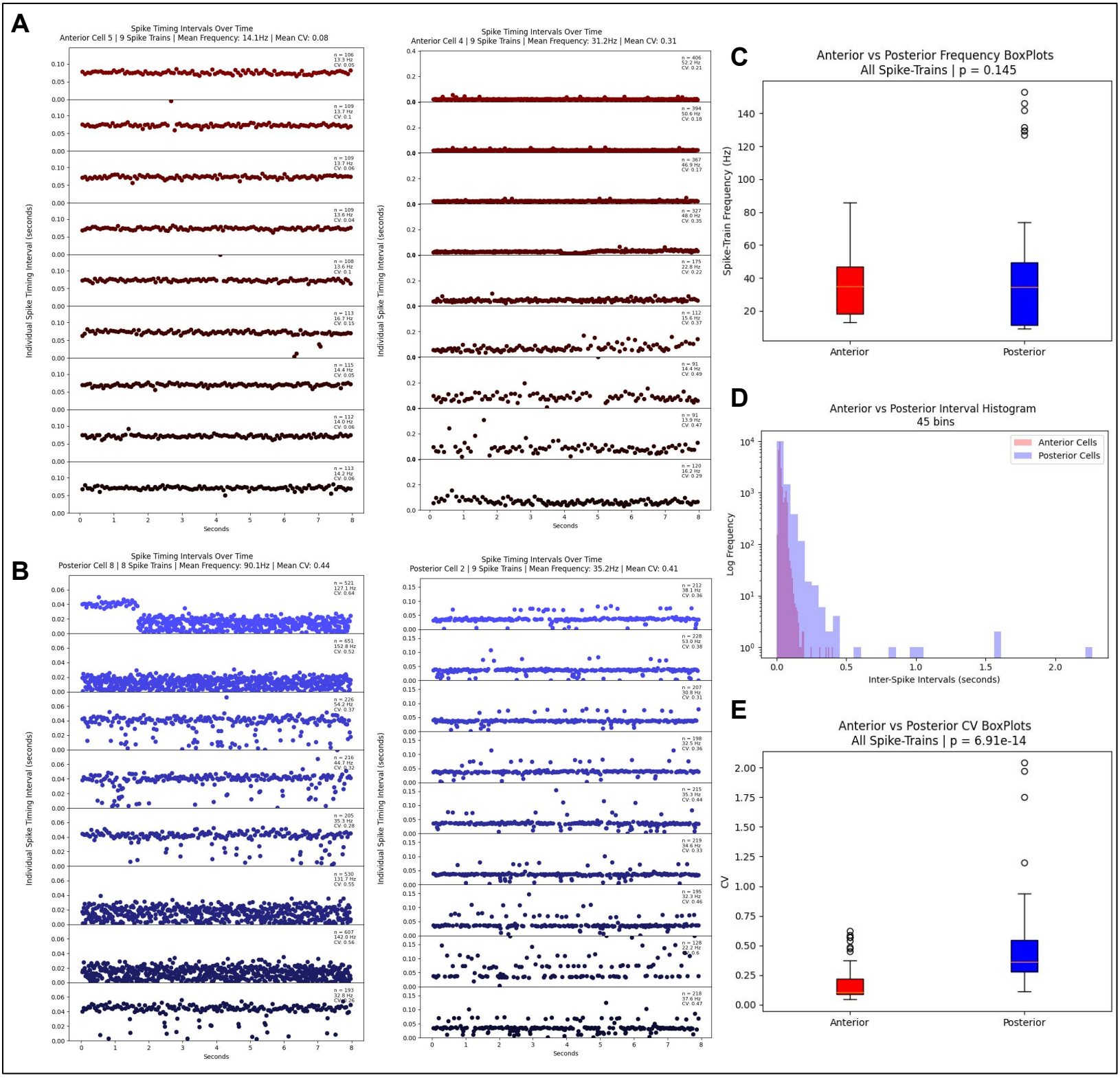

Figure 2. Inter-Spike Interval Analysis

(A) All inter-spike intervals in each unit's spike trains for two example anterior units. The number of spikes (n), mean train frequency in Hz and mean train CV are reported per spike-train. The overall mean frequency and CV are reported at the top of each plot. Each spike train is taken after the next, sometimes with a certain (unknown) delay. All anterior unit plots are shown in supplemental fig 1.
(B) All inter-spike intervals in each unit's spike trains for two example posterior units. The number of spikes (n), mean train frequency in Hz and mean train CV are reported per spike-train. The overall mean frequency and CV are reported at the top of each plot. Each spike train is taken after the next, sometimes with a certain (unknown) delay. All posterior unit plots are shown in supplemental fig 2.
(C) Frequency box plots of all spike trains for anterior vs posterior units. The Mann Whitney U test was run resulting in a non-significant p value of 0.145 between anterior and posterior data.
(D) Histogram representation of Inter-Spike Intervals from all spike trains of all cells in anterior (red) and posterior (blue).
(E) CV box plots of all spike trains for anterior vs posterior units. The Mann Whitney U test was run resulting in a significant p value of 6.91e-14 between anterior and posterior data.

Similarly, a significant difference was found between the per-spike train CV values of anterior and posterior cells (Figure 2E, Mann-Whitney U test: $p<<0.05$).

Many studies only report the dominant frequency of Purkinje cell firing as opposed to the more variable frequencies that can be observed on smaller time scales. As such, we were curious as to whether there was a difference between per neuron and per spike-train data. To visualize this, we plotted box plots of per-cell vs per-spike-train frequency and CV for both anterior and posterior cells (Supplementary Fig 3). We observed a non-significant difference between all per-cell and per-spike-train data within the anterior and posterior unit groups.

To visualize trends over both anterior and posterior populations, we plotted histograms of all inter-spike intervals (Figure 2D and detailed in Figures 3A and 3B). As per previous studies, the posterior unit histogram has a long tail absent from the anterior unit histogram. When plotted on the log scale (Figure 3C), we observe that the posterior histogram extends on either side of the anterior histogram (seen as the red and blue shaded regions delimited the anterior and posterior histogram ranges respectively).

The kernel density estimate (KDE) plot of both anterior and posterior inter-spike intervals resulted in three peaks, with the posterior KDE peaks occurring at lower normalized log values than those of the anterior units (Figure 3D). The two KDE plots had an overlap coefficient of 0.448 (values closer to 0 suggest no overlap while values closer to 1 suggest identical data distributions) and the skew of the KDE plot was 0.493 for the anterior units as opposed to -0.606 for the posterior units.

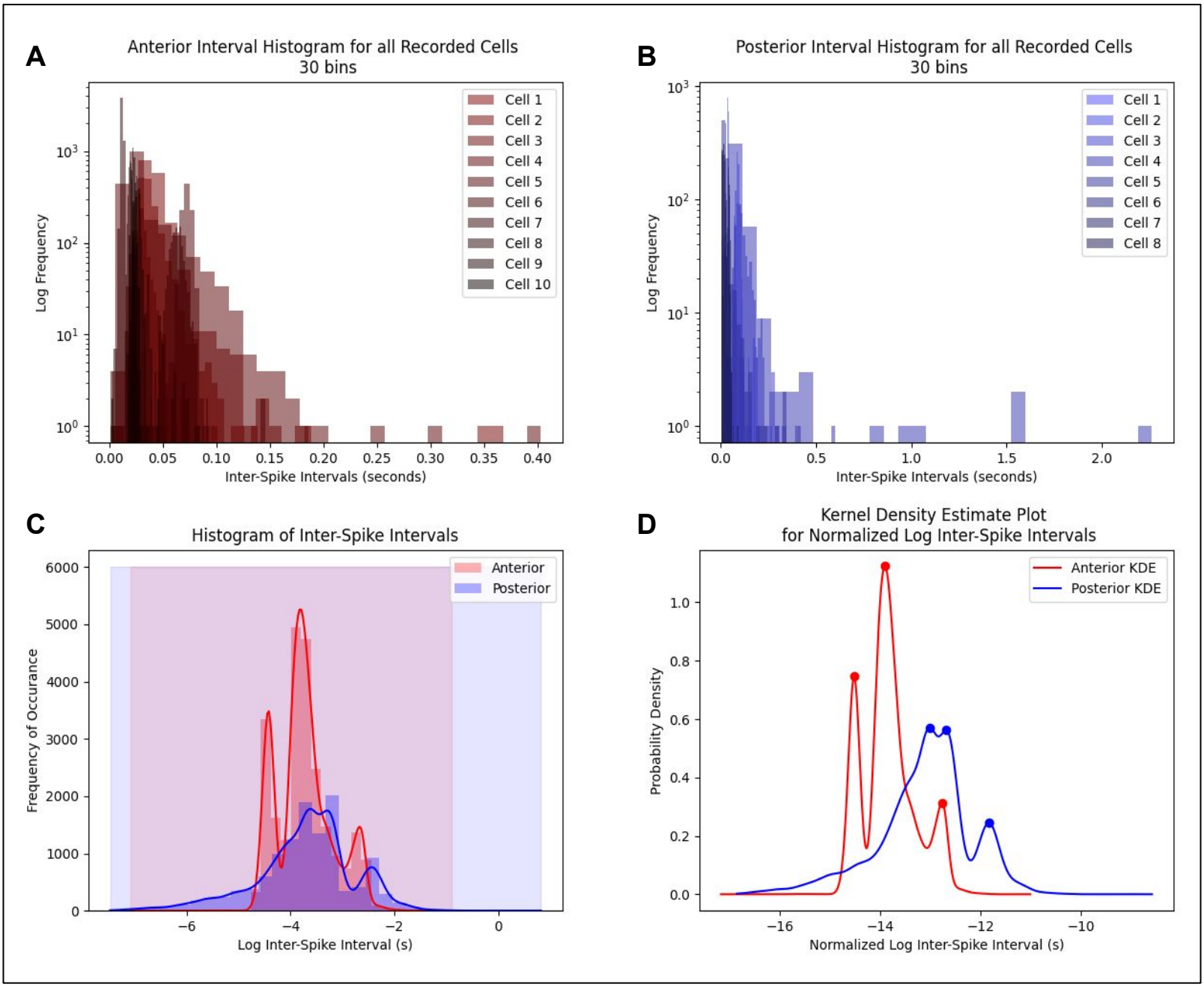

Figure 3. Histogram Analysis of Inter-Spike Intervals

(A) Log Histogram visualization of all 10 anterior cells. All inter-spike intervals for all cell trains were combined per cell. Cells that had lower numbers of spike trains (cell three with 6 spike trains) had wider bins compared to cells with more spike trains (10 trains max).
(B) Log Histogram visualization of all 8 posterior cells. All inter-spike intervals for all cell trains were combined per cell. Cells that had lower numbers of spike trains (cell four with 4 spike trains) had wider bins compared to cells with more spike trains (9 trains max).
(C) Anterior vs posterior inter-spike interval histograms. The red shaded portion of the graph shows the range of the anterior cell log inter-spike intervals while the blue shaded portion of the graph shows the range of the posterior cell log inter-spike intervals.
(D) Kernel density estimate (KDE) plot for anterior and posterior normalized log inter-spike intervals. The dots represent the peaks of the KDE curves.

Overall, our findings reveal a significant difference in the coefficient of variation between the anterior and posterior Purkinje cells and invite further investigation into regional differences in Purkinje cell firing patterns within the mammalian cerebellum.

Discussion:

Our study revealed a significant difference in the coefficient of variance between the firing frequency of Purkinje cells located in the anterior vs posterior vermis. Our findings, consistent with previous literature, suggest that the anterior zone of the vermis contains Purkinje cells with more regular firing patterns while the posterior zone hosts more irregularly firing Purkinje cells with a broader range of firing frequencies. The difference in regularity and predictability of Purkinje cell firing between anterior and posterior vermis zones suggest that different neural computations may be taking place as a result of differences in input and output, or due to a sequence of transformations that occur between the anterior and posterior regions in sequence. The specificity of the circuitry and connections between different zones of the cerebellum requires further research.

Purkinje cells exhibit simple and complex spiking patterns. Simple spikes (generally between 10-100Hz) arise intrinsically and are modulated by granule cells while complex spikes (less than 1Hz) are modulated by inputs from a single climbing fiber that connects to a single Purkinje cell through hundreds of synapses (Carey, 2024). From our study, the larger range of posterior Purkinje cell firing frequencies may suggest a greater propensity of these cells to produce complex spikes. Because

complex spikes involve the suppression or temporary pause of simple spiking, cells with relatively frequent complex spikes may have larger frequency CV values.

Intriguingly, our study found a stair-like inter-spike interval pattern observed in one anterior and one posterior Purkinje cell. This pattern, though uncommon in our data, is noteworthy due to its characteristic appearance and potential for transmitting two or more series of information at once. Computer modeling of this pattern would allow for a better understanding of the circuitry and underlying communication between the cerebellar zones and their corresponding outputs.

Certain posterior cells in our data also exhibited abrupt jumps in firing frequency, a phenomenon not observed in the anterior cells. While these are the result of in-vitro Purkinje cells that lack the majority if not all of their granule cell and climbing fiber inputs, future studies may find it interesting to measure the spike timing of several neighboring Purkinje cells to better determine the significance of these jumps and their capacity to carry information between cells cerebellar regions.

While our study provides valuable insights, certain aspects could be improved in future research. Notably, our study did not include the central zone of the vermis, which may have had an intermediate CV value to that of the anterior and posterior zones. Additionally, because our study was limited to discrete recording segments, we were unable to properly determine the frequency and CV over greater time scales. Despite the fast nature of cerebellar outputs, longer recordings may have allowed for the study of Purkinje firing patterns over time and within different groups or populations. Future studies may also benefit from simulating granule cells and climbing fiber inputs onto Purkinje cells using techniques such as optogenetics. These approaches would allow

for the manipulation of Purkinje inputs directly, providing a better overview of firing patterns under different conditions.

In conclusion, our study finds that anterior and posterior Purkinje cells in the rat vermis show differences in their firing patterns. Consistent with previous studies, we find that Purkinje cells in the anterior vermis have a smaller range of firing frequencies and a lower CV while those of the posterior vermis have larger frequency ranges and higher CV values. The distinct firing patterns of Purkinje cells in the anterior and posterior vermis may provide insight into the ability of the cerebellum to contribute to diverse behavioral and cognitive functions. Continued exploration of these patterns will allow us to gain a greater comprehension of cerebellar computations and their role in disease.

Supplementary Figures:

Supplemental Fig. 1: Anterior spike-train visualization per unit

Supplemental Fig. 2: Posterior spike-train visualization per unit

Supplemental Fig. 3: Per cell vs per spike-train analysis

Resource availability:

<table>
<tr><td colspan="2"><u>Data and code availability</u>: All original code and data are in GitHub and publicly available as of April 2024 and can be accessed through the following link: https://github.com/BruneBettler/BIOL-389-Purkinje

<u>Statistical Analysis:</u> All statistical tests used the Mann Whitney U Test completed on Python with the scipy.stats library unless specified otherwise.</td></tr>
<tr><td colspan="2"><u>Experimental model and subject details</u>: P18 - P25 Rats</td></tr>
<tr><td><u>Hardware and behavior setup</u>:
- Multiclamp 700B amplifier
- Upright microscope</td><td><u>Software</u>:
- Igor Pro 8.0
- Python</td></tr>
</table>

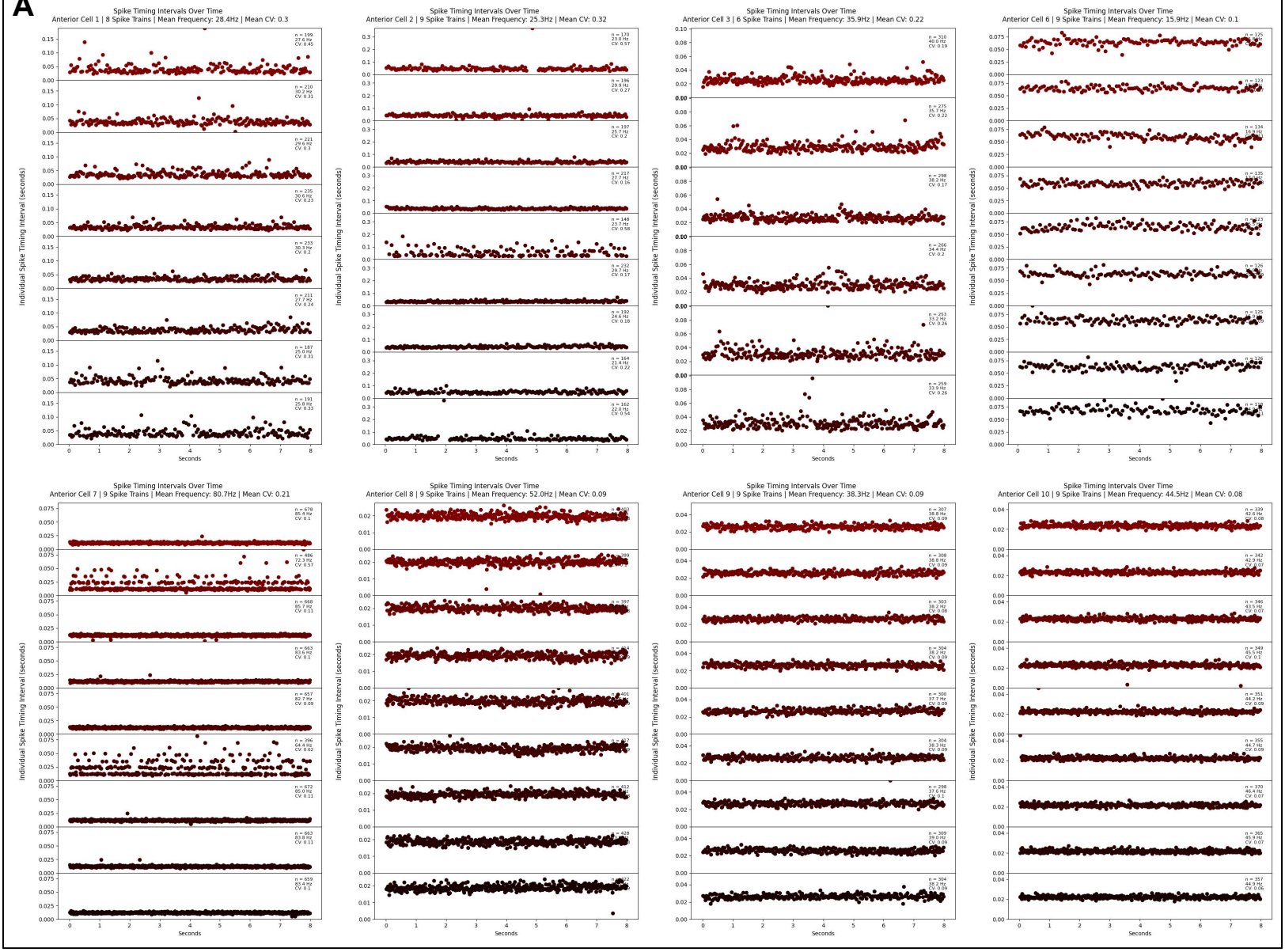

Supplemental Fig. 1. Anterior spike-train visualization per unit

(A) Inter-spike interval per spike-train per remaining unit not shown in Figure 2.

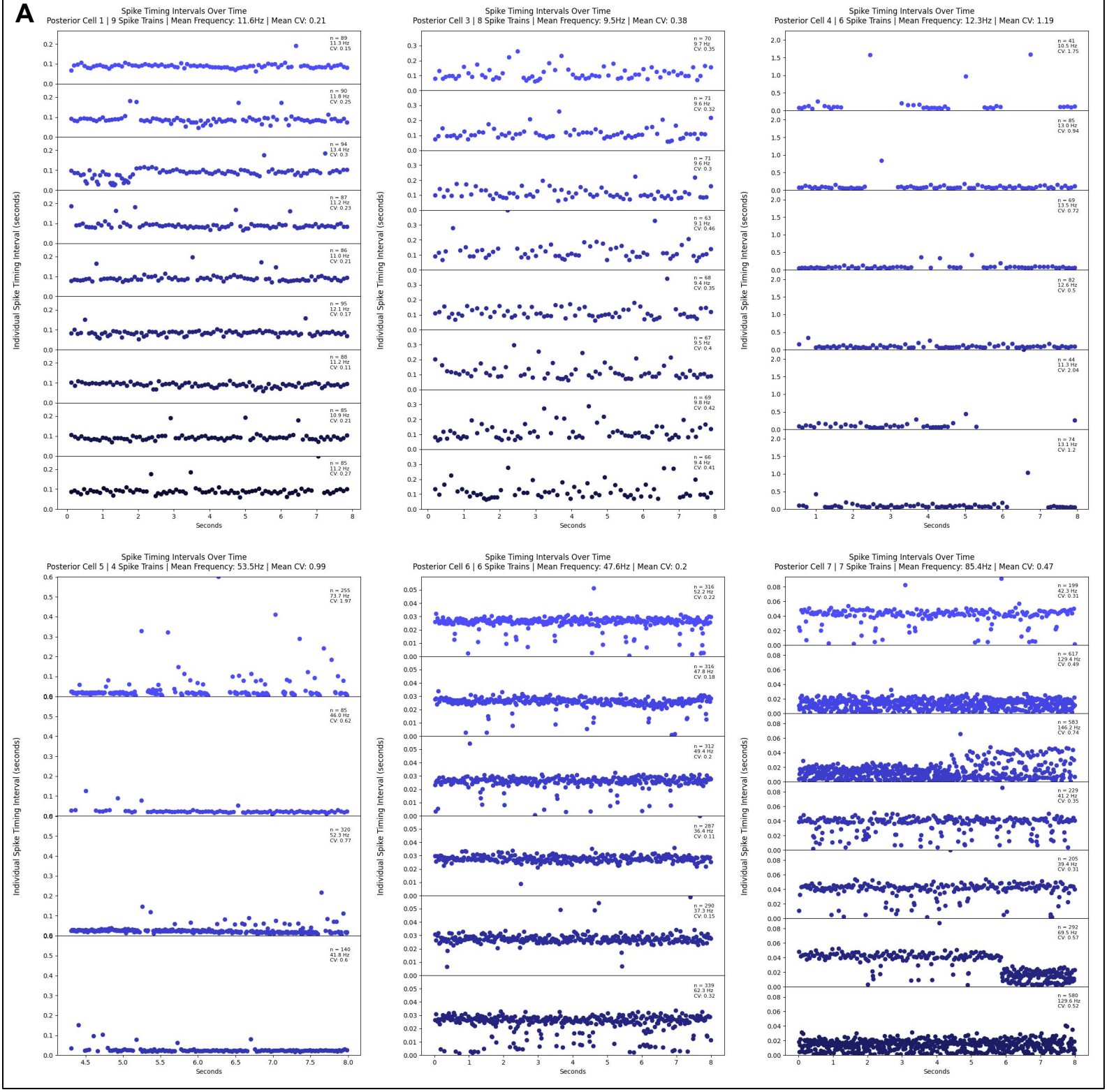

Supplemental Fig. 2. Posterior spike-train visualization per unit

(A) Inter-spike interval per spike-train per remaining unit not shown in Figure 2.

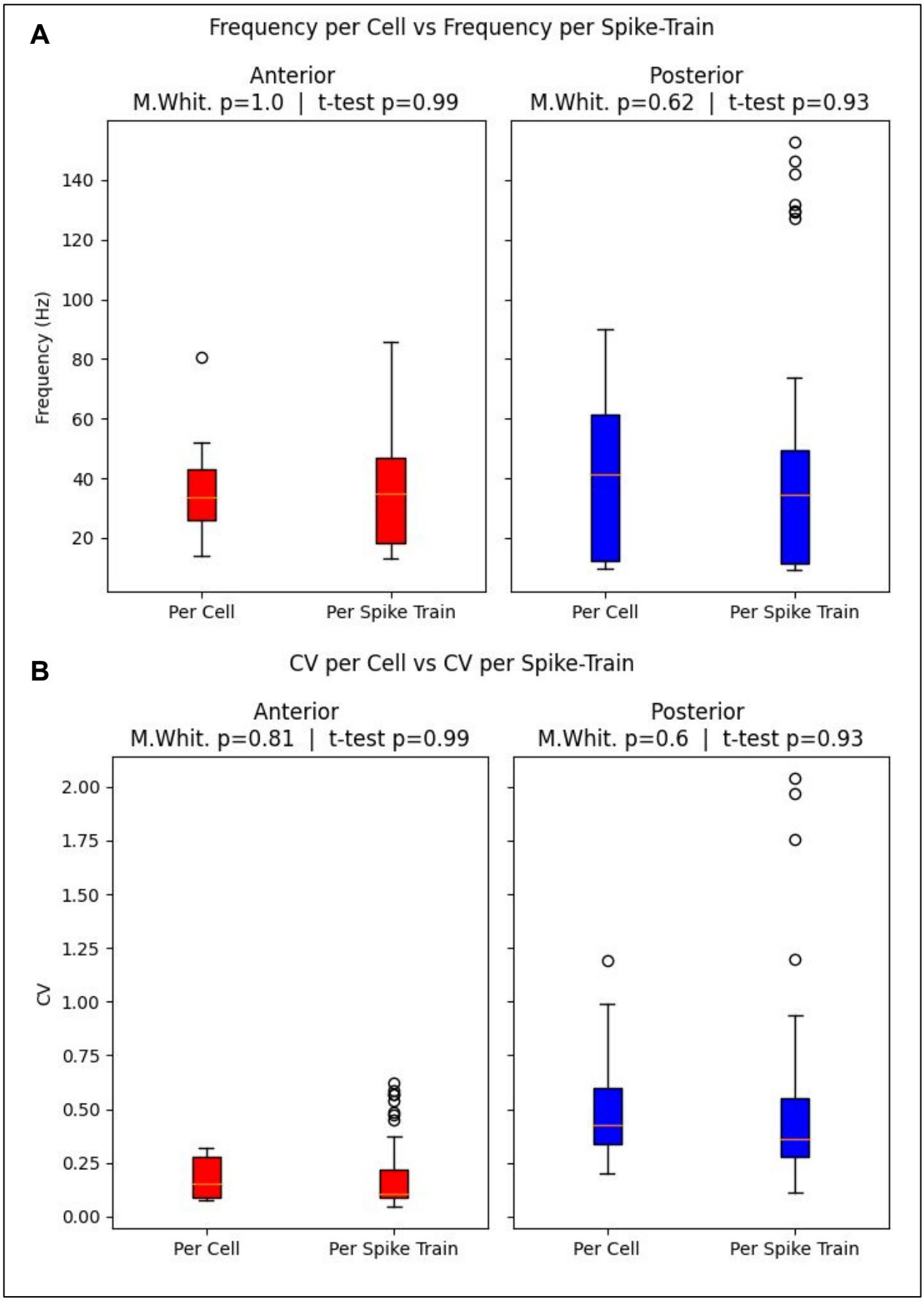

Supplemental Fig. 3. Per Cell vs Per Spike-Train Analysis

(A) Per cell dominant frequency vs per spike-train mean frequency box plots for both anterior (red) and posterior (blue) units. Both the Mann Whitney U and t-tests resulted in a non significant p value between per-cell and per spike-train for both anterior and posterior units.
(B) Per cell dominant CV vs per spike-train mean CV box plots for both anterior (red) and posterior (blue) units. Both the Mann Whitney U and t-tests resulted in a non significant p value between per-cell and per spike-train for both anterior and posterior units.

References:

Carey, M. R. (2024). The cerebellum. *Current Biology*, *34*(1), R7–R11. https://doi.org/10.1016/j.cub.2023.11.048

Coffman, K. A., Dum, R. P., & Strick, P. L. (2011). Cerebellar vermis is a target of projections from the motor areas in the cerebral cortex. *Proceedings of the National Academy of Sciences of the United States of America*, *108*(38), 16068–16073. https://doi.org/10.1073/pnas.1107904108

Cook, A. A., Fields, E., & Watt, A. J. (2021). Losing the Beat: Contribution of Purkinje Cell Firing Dysfunction to Disease, and Its Reversal. *Neuroscience*, *462*, 247–261. https://doi.org/10.1016/j.neuroscience.2020.06.008

Diedrichsen, J., King, M., Hernandez-Castillo, C., Sereno, M., & Ivry, R. B. (2019). Universal Transform or Multiple Functionality? Understanding the Contribution of the Human Cerebellum across Task Domains. *Neuron*, *102*(5), 918–928. https://doi.org/10.1016/j.neuron.2019.04.021

Hernández-Pérez, C., Weruaga, E., & Díaz, D. (2023). Lobe X of the Cerebellum: A Natural Neuro-Resistant Region. *Anatomia*, *2*(1), Article 1. https://doi.org/10.3390/anatomia2010005

Lehman, V. T., Black, D. F., DeLone, D. R., Blezek, D. J., Kaufmann, T. J., Brinjikji, W., & Welker, K. M. (2020). Current concepts of cross-sectional and functional anatomy of the cerebellum: A pictorial review and atlas. *The British Journal of Radiology*, *93*(1106), 20190467. https://doi.org/10.1259/bjr.20190467

Sultan, F., & Glickstein, M. (2007). The cerebellum: Comparative and animal studies. *The Cerebellum*, *6*(3), 168–176. https://doi.org/10.1080/14734220701332486

Toscano Márquez, B., Cook, A. A., Rice, M., Smileski, A., Vieira-Lomasney, K., Charron, F., McKinney, R. A., & Watt, A. J. (2021). Molecular Identity and Location Influence

Purkinje Cell Vulnerability in Autosomal-Recessive Spastic Ataxia of Charlevoix-Saguenay Mice. *Frontiers in Cellular Neuroscience*, *15*, 707857. https://doi.org/10.3389/fncel.2021.707857

Unverdi, M., & Alsayouri, K. (2024). Neuroanatomy, Cerebellar Dysfunction. In *StatPearls*. StatPearls Publishing. http://www.ncbi.nlm.nih.gov/books/NBK545251/

Welniarz, Q., Worbe, Y., & Gallea, C. (2021). The Forward Model: A Unifying Theory for the Role of the Cerebellum in Motor Control and Sense of Agency. *Frontiers in Systems Neuroscience*, *15*. https://doi.org/10.3389/fnsys.2021.644059

Wright, J. (2015, October 20). *Differences between rodents show limitations of models*. Spectrum | Autism Research News.